HOT ROCKS! NEAR-INFRARED REFLECTANCES (AND EMISSIVITIES) OF ROCKS AT VENUS SURFACE TEMPERATURES.

A. H. Treiman[1], J. Filiberto[1], K.E. Vander Kaaden[2]. [1]Lunar and Planetary Institute, USRA, 3600 Bay Area Blvd. Houston TX 77058 <treiman@lpi.usra.edu>. [2]Jacobs, NASA Johnson Space Center, Mail Code XI3, Houston, TX 77058.

Introduction: Venus' surface can be viewed in emission through a few near-infrared (NIR) spectral 'windows' (1 μm) in its relatively opaque atmosphere [1]. Venus' surface shows NIR emissivities that correlate with surface geology [2-4], and these emissivity variations are interpreted as differences in surface rock type (mafic vs. silicic) and/or extent of weathering (Fe^{2+} silicates vs. Fe^{3+}-oxide-coated).

To understand and quantify the observed variations in NIR emissivity, high-temperature (T) emissivity can be measured directly [5,6]. For example, emissivities of basalts in the wavelength range $0.85 - 1.2$ μm are ~0.95 [5-8]. This can be tested by measureing reflectance, because Kirchoff's Law holds that emissivity (**e**) = 1 – reflectance (**r**). The **r** of basalt in the NIR is ~0.05 [o] consistent with a NIR **e** of ~0.95 [5-8].

High-T NIR **e**'s of silicic igneous rocks (granitic, rhyolite) have been reported to be 0.8-0.9 [5,6], which is inconsistent with **r** values of 0.3-0.8 of such rocks at 25°C [9,10]. However, these measurements have been updated [7,8] and are consistent with the results here (see below and Fig. 3).

Samples & Methods: We measured reflectances of rough surfaces of: alkali basalt, tholeiite, and dunite (Spitsbergen, Norway); granite (Mt. Lowe, San Gabriel Mts., CA); hematite-coated basalt cinder (Vesuvius, Italy); dacite (Mt. Hood, CA), sandstone (Entrada ss., UT), and hematite (Soudan, MN). Standards were rods of polycrystalline MgO and graphite, with estimated **r**'s of 0.8 and 0.05 respectively [11,12]. **r** values at 25°C ($350 - 2500$ nm) were measured <u>first</u> with a Spectral Evolution OreXpress Spectrometer using its contact reflectance probe, i.e. a phase angle φ of near zero.

Reflectances at ~470°C were measured in two modes, on samples and standards in a box furnace (Figure 1). Illumination was from LED flashlights of nominal 850 and 940 nm. Imaging was with a pocket digital camera that had been modified to pass NIR light. Its charge-coupled device (CCD) image plane is not sensitive to light of wavelength longer than ~1000 nm. Images were taken through a 850 nm band-pass filter (25 nm pass) and 900 nm long-pass filter. Average digital numbers (DN) were taken from the camera's JPG images; DN were converted to **r** values by interpolating between the standards' DNs, after calculating (and undoing) the camera's γ-correction. γ=1.5 yielded an adequate relationship between pixel DN and **r** values from a photographic gray card (LED flashlights at 25°C).

In the first mode, samples were viewed through the

Figure 1. Rocks and standards at ~470°C, imaged in ~940 nm light. Rocks (clockwise from left) are: tholeiite basalt, granite, hematite-coated basalt cinder. Black and white rods are graphite and MgO standards. DN here used for Figure 2.

furnaces gas exit port, with the furnace door closed. Illumination was also through the exit port, with a polka-dot beam-splitter allowing both illumination and imaging through the port (i.e., φ = 0°). In the second mode, samples were heated to ~500°C in a closed furnace; then the door was opened and images taken immediately. Rock temperatures were near 470°C, and φ = ~90°.

Conclusion: Our results (Fig. 2) are informative, if preliminary. Temperatures were approximate, viewing geometry varied, standard reflectances are approximate, and light sources and detector were far from ideal.

With these caveats, **r** values for most rocks at ~470°C are close to those at 25°C (Fig. 2). The differences between measured **r** values can be ascribed to: viewing geometry (φ = 0° at 25°C; ~90° at 470°C); differences in mineral proportions analyzed in coarse-grained rocks; chemical reactions during analysis; and uncertainties in the high-temperature values. Some basalts developed thin coating of hematite during heating, which accounts for some increases in **r**. The measured **r** for dunite is comparable to that of olivine at high T [13,14]. In NIR images, the dunite is nearly as dark as the enclosing basalt, because 850 and 940 nm are in olivine's major absorption band. Hematite at ~470°C has lower **r** than at 25°C. This is because hematite's red absorption edge diminishes and shifts to longer wavelength with temperature. To the naked eye, hematite powder is red at 25°C and brown at ~470°C [15,16].
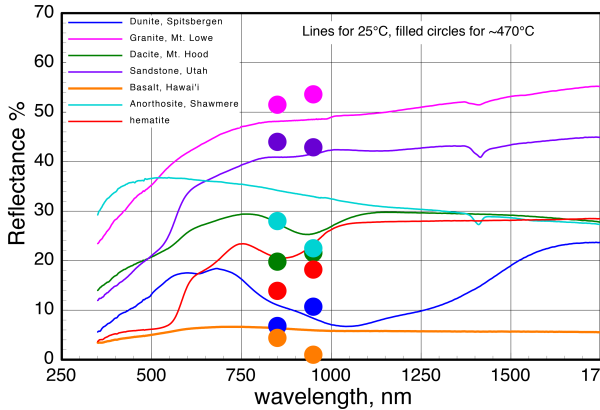
Figure 2. Rock reflectances at 25°C (lines) and at ~470°C (circles), coded to identical colors. To first order, reflectances at high T are similar to those at room T.

Following Kirchoff's Law, one can calculate NIR emissivities **e** for rocks at Venus surface T from **r** at that T. Results here imply that silicic igneous rocks (e.g., granite, dacite) on Venus will have **e** values of 50-80% (Fig. 3), similar to the most recently reported **e** [7,], but far lower than in earlier reports [5,6]. These lower **e** values for silicic igneous rocks are quite distinct from those of basaltic rocks, and imply that most crystalline silicic rock should be readily distinguishable from basaltic rock in NIR emissivity measurements from orbit.

Some silicic igneous rocks have low **r**, and are thus likely to exhibit high **e** values on Venus' surface. Typically, such rocks consist of dispersed small opaque particles in a relatively transparent matrix, like rhyolitic obsidian [5,6] and some larvikite 'granite.' The high **e** of such rocks may be misleading.

In the absence of **e** or **r** measurements at Venus surface T, **r** values at 25°C are reasonable predictors of high temperature **r** and **e** values (Fig. 2). For example,

one can predict that quartz sand (NIR **r** of ~0.65 at 25°C [17]) would have a Venus-T **e** of ~0.35, comparable to the measured value [7]. Likewise, anhydrite ($CaSO_4$) on Venus should have low **e**, possibly as low as 0.1 [18].

Thus, NIR emissivity at high T can be estimated (to first order) from reflectance at room T, and NIR emissivity alone cannot definitively distinguish silicic from basaltic igneous rock.

References: [1] Meadows V.S. & Crisp D. (1996) *JGRP 101*, 4595-4622. [2] Hashimoto G.L. et al. (2008) *JGRP 113,* E00B24. [3] Mueller N. et al. (2008) JGRP *113*, E00B17. [4] Gilmore M.S. et al. (2015) *Icarus 254*, 350-361. [5] Helbert J. et al. (2017) *LPSC* 48th, Abstr. #1512. [6] Dyar M.D. et al. (2017) *VEXAG 15th.* Abstr. & Presentation. [7] Dyar M.D. et al. (2019) VEXAG Presentation to *Planetary Science Advisory Committee* of NRC. Page 14 of Presentation. [8] Dyar M.D. et al. (2019) AGU abstract P14B08. [9] Adams J.B. & Filice A.L. (1967) *JGR 72*, 5705-5715. [10] Baird A.K. (1984) *JGR 89* 2491-2496. [11] Modest M.E. (1999) Heat and Mass Transfer: Radiation, Ch. 3 in Kreith F. ed., *CRC Handbook of Thermal Engineering*. Boca Raton La. [12] Touloukian Y.S. & DeWitt D.P. (1972) Thermal Radiative Properties - Nonmetalllc Solids, Vol. 8 in Touloukian Y.S. ed., *Thermophysical Properties of Matter*. TPRC, Purdue Univ. [13] Singer R.B. (1981) JGR 86,7967-7982. [14] Izenberg N.R. et al. (2014) *EPSC Abstr.* 9, EPSC2014-776-1. [15] Pieters C.M. et al. (1986) *Science* 234, 2379-2383. [16] Yamanoi Y. et al. (2009) *Amer. Mineral* 94, 90-97. [17] Hovis W.A. (1966) *Applied Optics* 5, 245-248. [18] Bishop J. et al. (2014) *Amer. Mineral*. 99, 2105-2115.
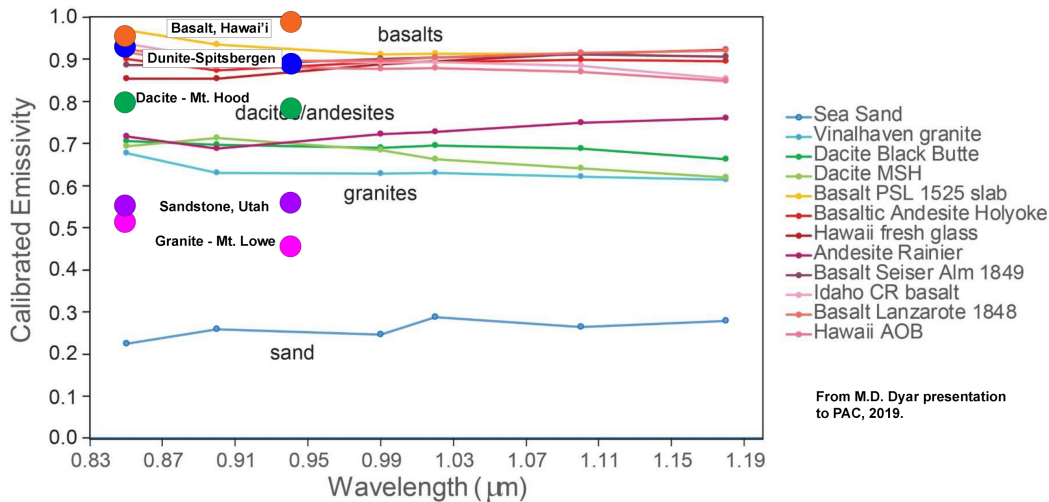

Figure 3. Rock emissivities **e** calculated from reflectances **r** at ~470°C, large filled circles colored as in Fig. 2. Lines and small circles are measured **e** values [7]. Base image from [7].